Biophysical Journal, Volume 97

**Supporting Material**

# Human Serum Albumin Inhibits Aβ Fibrillization through a 'Monomer-Competitor' Mechanism

Julijana Milojevic, Annie Raditsis, and Giuseppe Melacini

# Supplementary Material

# For

# Human Serum Albumin Inhibits Aβ Fibrillization through a 'Monomer-Competitor' Mechanism

*Julijana Milojevic, Annie Raditsis and Giuseppe Melacini**

Departments of Chemistry, Biochemistry and Biomedical Sciences
McMaster University, 1280 Main Street West, Hamilton, Ontario, L8S 4M1, Canada

E-Mail: melacin@mcmaster.ca

**Sample Preparation Protocols:**

*Aβ (12-28) Samples.* The Aβ (12-28) peptide used in this investigation was purchased from EZBiolab Inc., with a purity greater than 95 %. 1 mM and 0.7 mM Aβ (12-28) solutions were prepared by dissolving the peptide as a lyophilized powder in 50 mM acetate buffer–$d_4$ at pH 4.7, with 10% $D_2O$. This buffer composition was used because it has been previously shown to stabilize the monomeric and early oligomeric forms of the Aβ (12-28) peptide (11, 16, 17). In order to remove aggregates formed during the peptide lyophilization and dissolution processes, the peptide solution was filtered through a Ultrafree-MC Millipore 30 kDa cutoff filter in 5 min intervals at 3,000 rpm. To maximize and stabilize the monomeric form of the peptide, the filtered 0.7 mM Aβ (12-28) sample was diluted to 0.2, 0.1 and 0.025 mM concentrations with 50 mM acetate buffer–$d_4$ at pH 4.7 and 10% $D_2O$ and was used in the NMR and fluorescence measurements.

*Aβ (1-40) and Aβ (1-42) Samples.* The Alzheimer's peptides Aβ (1-40) and Aβ (1-42) were purchased from EZBiolab Inc., with a purity greater than 95 %. 1 mg of either Aβ peptide was initially dissolved in 500 μL of ice cold 10 mM NaOH. After dissolution, the sample was sonicated for 2 min and then it was placed on ice for 2 min. This sonication/cooling cycle was repeated twice. Aliquots taken from this stock solution were diluted in 20 mM potassium phosphate buffer at pH 7.4, 10 % $D_2O$ and 0.02 % $NaN_3$ resulting in 100, 90 and 25 μM peptide solutions. Aggregated 100 and 90 μM Aβ(1-42) peptide samples were prepared by incubating the Aβ (1-42) solution in a water bath at 37 $^oC$ for 3 hours without mixing.

*Other Samples.* L-Tryptophan and aspirin were purchased from Sigma-Aldrich. A 0.2 mM aspirin solution was prepared through serial dilutions of a 2 M aspirin stock DMSO solution with 50 mM acetate buffer–$d_4$ at pH 4.7, with 10 % $D_2O$. In the final solution DMSO was present at a residual concentration of 0.01 %. A 0.2 mM tryptophan solution was prepared through direct dissolution of the dry powder in acetate buffer. Fatty acid free and essentially globulin free HSA was purchased from Sigma with a 99 % purity. 1 mM stock solutions were prepared by dissolving HSA in the buffers used for the spectroscopic analyses.

**Optimization and Controls for STD Experiments**

In order to maximize the sensitivity of the STD experiments, we have first optimized the on-resonance frequency of the STD Gaussian pulse train for maximal HSA saturation. To monitor the degree of HSA saturation as a function of selective irradiation frequency, STD spectra were acquired for a concentrated HSA solution (*i.e.* 0.5 mM) using a short spin-lock (*i.e.* 100 μs) and setting the carrier frequency of the saturating Gaussian pulse train at offsets of -0.26, 0.57, 0.66, and 7.05 ppm (Fig. S1). Figure S1 indicates that saturation in the -0.26 – 0.66 ppm range results in optimal and thorough saturation, with STD spectra resembling the reference spectra (STR) acquired under the same experimental conditions. Figure S1 also reveals that saturation of the aromatic region results in less efficient spin diffusion as shown by a lower STD signal of the methyl region relative to the saturated spectral region. We therefore selected a 0.66 ppm saturation frequency for all subsequent STD experiments.

Before applying the STD experiments to the Aβ systems, we tested the sensitivity of our STD experiments to interactions in the μM – mM range using known control HSA ligands, *i.e.* aspirin and L-tryptophan. Aspirin binds with an overall dissociation constant ($K_D$) of ~70 μM to

Sudlow sites I and II, located in the HSA subdomains IIA and IIIA, respectively (26), while L–tryptophan binds with a ~mM $K_D$ to Sudlow site II under our experimental conditions (25). We therefore acquired saturation transfer difference (STD) and reference (STR) spectra for both aspirin and L-tryptophan in the absence (Fig. S2a, e) and in the presence of HSA at different concentrations (Fig. 2b-d and 2f-h). Without HSA no STD signal is observed (Fig. S2a, e) proving that the STD signal is a result of protein- ligand interactions only. As 1 μM HSA is added, a detectable STD signal is apparent for aspirin with μM affinity (Fig. S2b) but not for L-tryptophan with mM affinity (Fig. S2f). As the concentration of HSA increases to 10 μM the STD signal of aspirin builds up (Fig. S2c) but further addition of HSA causes line-broadening for the aspirin resonances with consequent loss of signal (Fig. S2d). Unlike aspirin, the STD signal of L-tryptophan is detected only at 100 μM but not at 10 μM HSA, due to the lower affinity for HSA of L-tryptophan (Fig. S2g, h). Overall, the control experiments of Fig. S2a-h prove that the STD spectra acquired under our experimental conditions are efficient at probing HSA interactions within a wide $K_D$ range, provided that the STD and STR data are acquired at several HSA concentrations.

**Test of the Model II ("Dissociation Catalyst" Model) using Aβ (12-28)**

The 1D-NMR spectrum of monomeric Aβ (12-28) prepared through filtration (Fig. S5a) was acquired first as a reference. This 1D trace is characterized by narrow line-widths as expected for a 17 amino acid peptide in which the self-association equilibria are largely shifted towards the monomeric form. However, upon addition of 25 mM NaCl to the filtered Aβ (12-28) sample a marked increase in linewidths is observed for most resonances after an equilibration time of seven days (Fig. S5b). The salt-induced line-broadening is a result of the hydrophobic-collapse driven oligomerization promoted by the higher ionic strength, which weakens electrostatic inter-molecular repulsions (15). For the Aβ (12-28) system the NMR line-width is therefore a convenient qualitative indicator of self-association (11, 15-17). Upon addition of 10 μM HSA to the Aβ (12-28) sample with 25 mM NaCl a marked overall line-narrowing is detected (Fig. S5c), as previously observed (11), confirming that HSA interferes with the exchange of polypeptide chains between the monomeric and the oligomeric states of Aβ (12-28). However, while albumin addition sharpens several peaks to line-widths comparable with those of the filtered sample (Fig. S5a, c), it does not restore the NMR signal intensities to those observed for the original filtered Aβ (12-28) sample before the salt-induced oligomer formation (Fig. S5a). Similar conclusions are reached even with different window function-induced line broadening (Fig. S6a), proving that the intensity differences between panels a and c of Fig. S5 are not an artifact of the specific apodization shape used. Furthermore, the intensity loss observed in the presence of protein (Fig. S5c) cannot be explained by direct salt effects on the sensitivity of the cryoprobe as the residual glycerol signal from the filter does not change significantly in the presence of salt (Fig. S6b). These experiments therefore show that although albumin prevents monomer/oligomer exchange it does not dissociate oligomers into monomers. The significantly lower population of the monomeric state in the samples with HSA (Fig. S5c) relative to the control solution (Fig. S5a) is therefore in agreement with the conclusion reached for Aβ (1-42) (Fig. 6).

**Effect of HSA on the mechanism of homogenous nucleation – growth**

A better appreciation of how HSA kinetically controls the Aβ fibrilization can also be obtained in light of a previously proposed model for the homogeneous nucleation/growth of Aβ fibrils (31). Accordingly to this model, nuclei are first formed through the reversible self-association of monomeric peptides into micellar aggregates. These peptidic micellar nuclei serve as seeds for the growth of fibrils through the largely irreversible addition of monomeric peptides. Based on this fibrillization mechanism, the main source of depletion of monomeric and low MW peptide aggregates is therefore the actual fibril growth. Albumin acts on the growth phase preventing the addition of monomeric peptide to the initially formed high MW oligomers and growing fibrils. The Aβ peptide remains then kinetically trapped in the thermodynamically unfavorable nucleation phase, where it exists in the monomeric form in equilibrium with low MW aggregates.

## Captions for Supplementary Figures

**Figure S1.** Effect of saturation frequency on the saturation transfer difference (STD) spectra of a 0.5 mM HSA sample. The bottom panel reports the reference spectrum (1D-STR) of the 0.5 mM HSA sample obtained with off resonance saturation at -30 ppm. Selective HSA saturation at 0.57, 0.66 and -0.26 ppm results in STD spectra similar to the reference STR spectra indicating complete saturation of the HSA at those frequencies. Saturation of the aromatic residues at 7.05 ppm does not provide complete saturation of the HSA molecule, resulting in higher signal intensity in the saturated aromatic region relative to other spectral regions. 0.5 mM HSA was prepared in 50 mM acetic acid–$d_4$ at pH 4.7. All spectra were recorded at 700 MHz using a TCI CryoProbe and at 20 $^{o}$C. A short 0.1 ms spin lock (SL) was used to maximize the HSA signal and spectra were processed using a line broadening factor of 3 Hz. Red arrows indicate the selective saturation frequency offsets.

**Figure S2.** Effect of HSA on the saturation transfer reference (STR) and saturation transfer difference (STD) spectra of aspirin, L-tryptophan. All ligand solutions were prepared at 0.2 mM concentration in 50 mM acetic acid-$d_4$, pH 4.7, 10% $D_2O$. The STR and STD spectra of 10 and 100 μM HSA solutions were subtracted from the protein ligand mixture spectra to remove potential residual HSA signal. In addition, a 30 ms long spin lock (SL) was used to minimize the residual HSA signal. Aspirin was used to probe HSA interactions in the μM range, while L-Tryptophan at pH 4.7 is used to model HSA interactions with a $K_D$ in the mM range. All spectra were acquired at 700 MHz using a TCI CryoProbe and at 20 $^{o}$C. All spectra were processed using a line broadening factor of 3 Hz.

**Figure S3.** Effect of pH on the maximum emission wavelength of the HSA tryptophan fluorescence as a monitor of the structural transitions of albumin (22). Experiments were performed at 20 °C with a 5 μM HSA concentration in 50 mM sodium acetate buffer. Different pH values were obtained by adding 0.1 M NaOH or HCl solutions. Each spectrum was recorded at least three times and the average maximum wavelength ($\lambda_{max}$) values were plotted against pH. The error was calculated as the standard deviation of all $\lambda_{max}$ values at each pH. pH ranges assigned to different inter-domain orientations of albumin are marked in different colors.

**Figure S4.** Albumin interacts with Thioflavin T. Panel (a) and (b) report the STR spectra of a 1 mM ThT solution in 50 mM sodium acetate buffer, pH 4.7, 10% $D_2O$ in the absence and presence of 20 μM HSA, respectively. Panel (c) and (d) report the corresponding STD spectra for ThT in the absence and presence of 20 μM HSA, respectively. Experiments were acquired using a Bruker AV600 spectromete at 20 $^{o}$C.

**Figure S5.** Effect of HSA on the 1D–NMR spectra of the Aβ (12-28) peptide. Panel **(a)** reports the spectrum of a 30 kDa filtered 1 mM Aβ (12-28) solution. Addition of 25 mM NaCl (panel **(b)**) causes significant aggregation as indicated by line broadening and intensity losses. Panel **(c)** shows the effect of the addition of HSA to the aggregated Aβ (12-28) sample. Red dotted lines and arrows were added to facilitate the comparison of the 1D intensities between different spectra and to show that although HSA addition results in line sharpening, it does not result in the restoration of the starting signal intensity. Experiments were recorded at 700 MHz using a

TCI CryoProbe and at 20 $^{o}$C. All spectra were processed using a line broadening factor of 0.3 Hz.

**Figure S6. (a)** The 1D NMR spectral expansion shown in black corresponds to the Aβ (12-28) filtered peptide solution without any salt or protein, while the trace in red shows the effect of the addition of 25 mM NaCl salt followed by the addition of 10 µM HSA. Both spectra were processed with a line broadening coefficient of 10 Hz. **(b)** The residual glycerol signal in the same spectra as in panel (a). The glycerol signal was used to test the probe performance under different salt conditions. No significant difference in the intensity of the glycerol signal was observed in the presence or absence of 25 mM NaCl, indicating that the salt addition did not compromise the probe performance.

# Figure S1

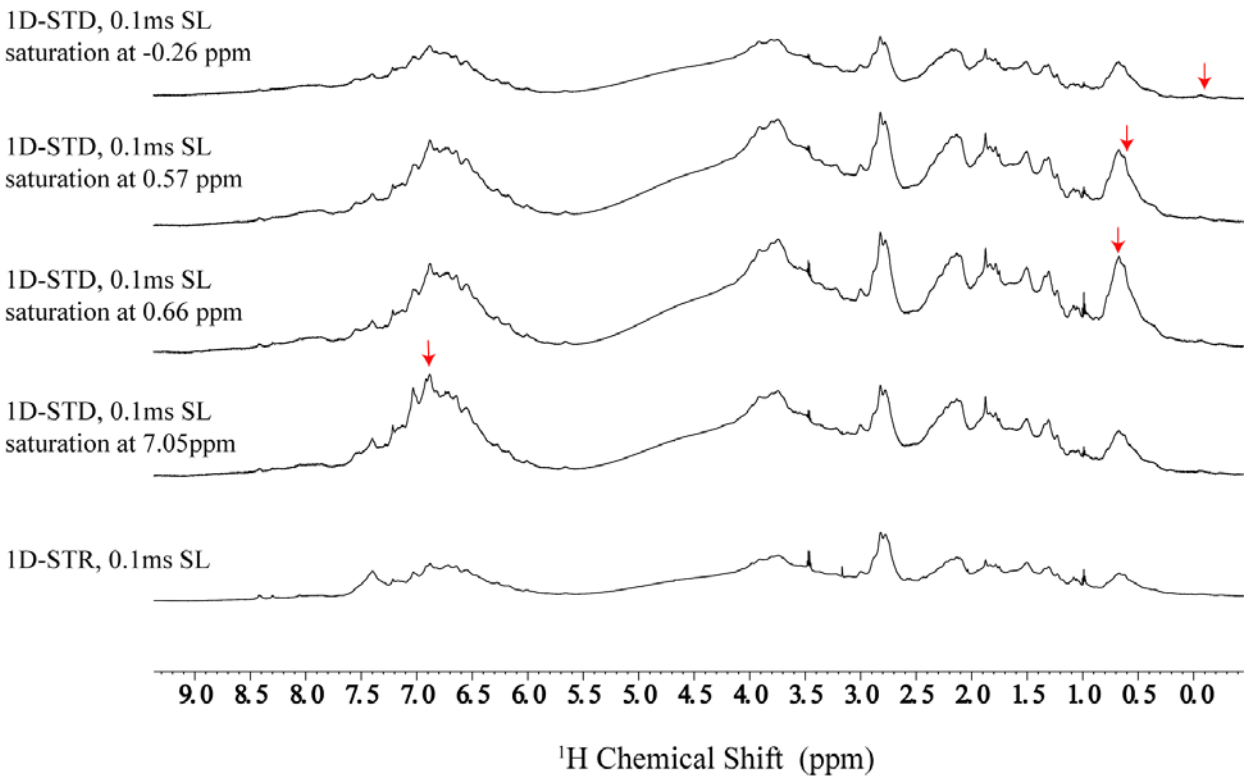
1D-STD, 0.1ms SL
saturation at -0.26 ppm
1D-STD, 0.1ms SL
saturation at 0.57 ppm
1D-STD, 0.1ms SL
saturation at 0.66 ppm
1D-STD, 0.1ms SL
saturation at 7.05ppm
1D-STR, 0.1ms SL
9.0 8.5 8.0 7.5 7.0 6.5 6.0 5.5 5.0 4.5 4.0 3.5 3.0 2.5 2.0 1.5 1.0 0.5 0.0
¹H Chemical Shift (ppm)

# Figure S2

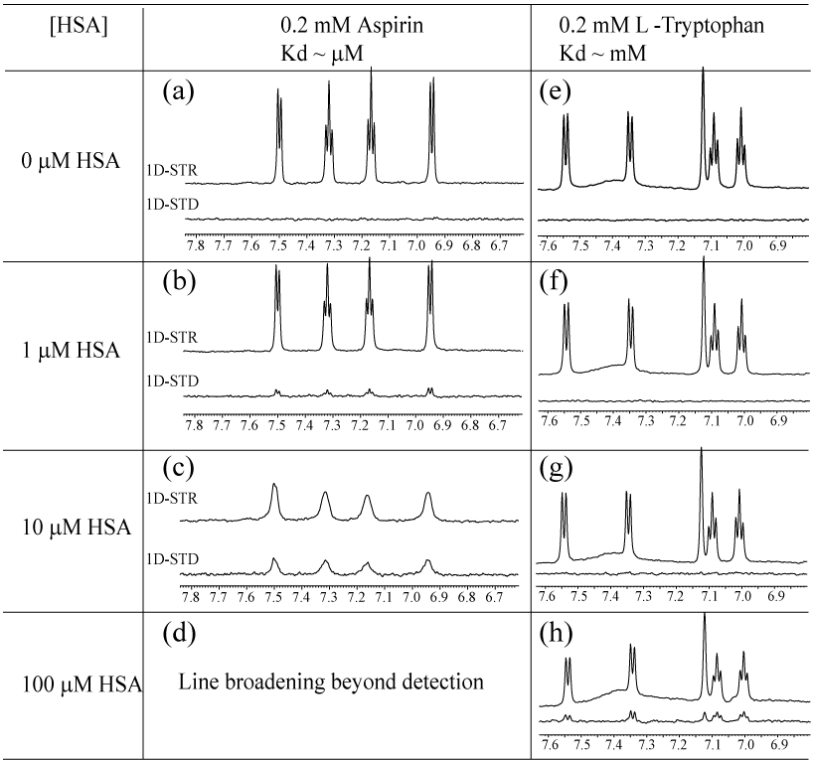
[HSA]
0.2 mM Aspirin
Kd ~ µM
0.2 mM L -Tryptophan
Kd ~ mM
0 µM HSA
1 µM HSA
10 µM HSA
100 µM HSA
(a)
(b)
(c)
(d)
(e)
(f)
(g)
(h)
1D-STR
1D-STD
Line broadening beyond detection
7.8 7.7 7.6 7.5 7.4 7.3 7.2 7.1 7.0 6.9 6.8 6.7
7.6 7.5 7.4 7.3 7.2 7.1 7.0 6.9

# Figure S3

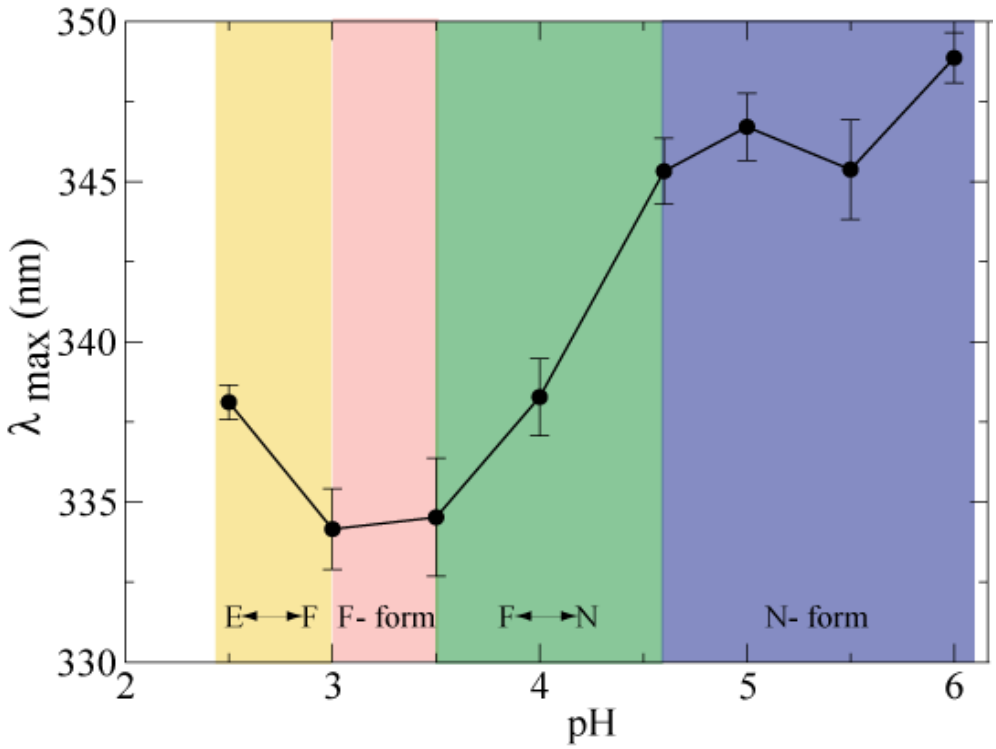

# Figure S4

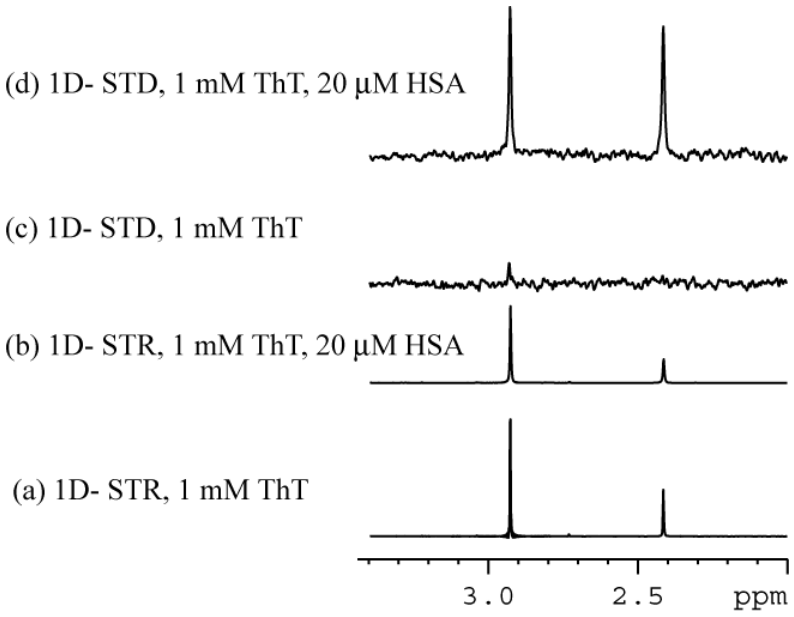
(d) 1D- STD, 1 mM ThT, 20 µM HSA
(c) 1D- STD, 1 mM ThT
(b) 1D- STR, 1 mM ThT, 20 µM HSA
(a) 1D- STR, 1 mM ThT
3.0
2.5
ppm

# Figure S5

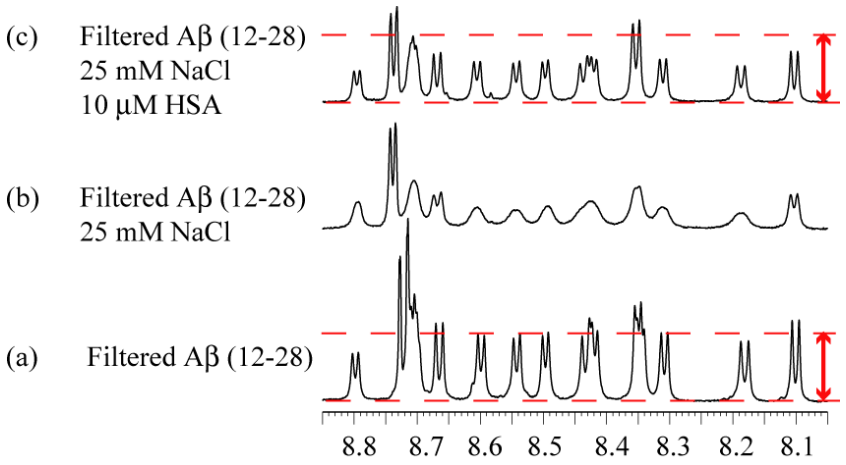
(c)
Filtered Aβ (12-28)
25 mM NaCl
10 µM HSA
(b)
Filtered Aβ (12-28)
25 mM NaCl
(a)
Filtered Aβ (12-28)
8.8
8.7
8.6
8.5
8.4
8.3
8.2
8.1

# Figure S6

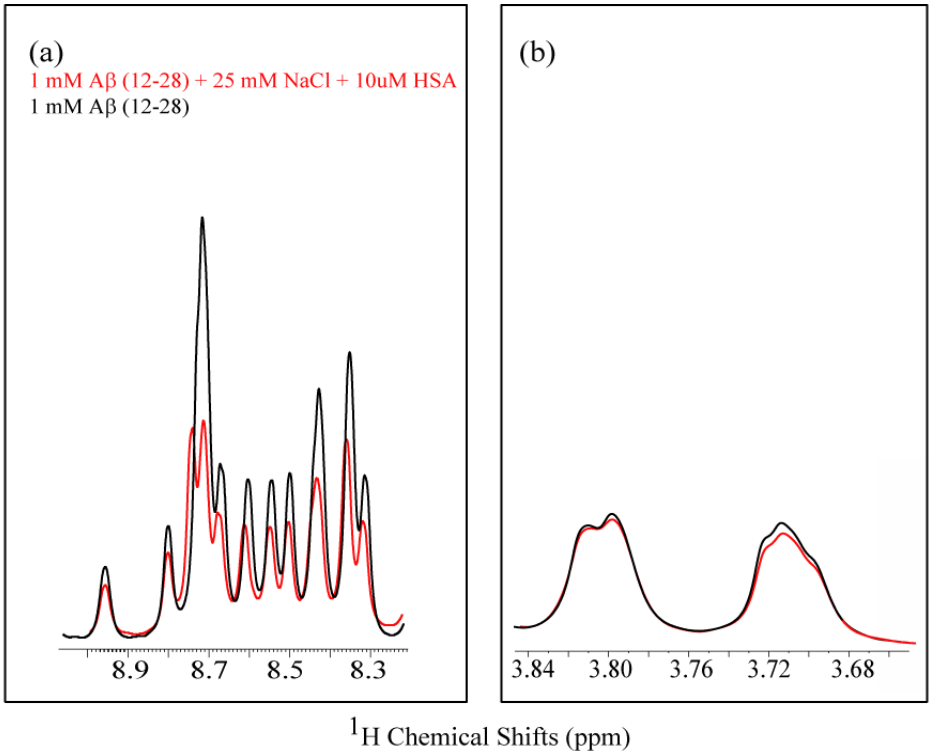
(a)
1 mM Aβ (12-28) + 25 mM NaCl + 10uM HSA
1 mM Aβ (12-28)
8.9
8.7
8.5
8.3
(b)
3.84
3.80
3.76
3.72
3.68
$^1$H Chemical Shifts (ppm)